T.1: Physics of Semiconductor Optoelectronic Devices Indigenously Developed at RRCAT

V. K. Dixit
Semiconductor Material Laboratory
Materials Science Section
E-mail: dixit@rrcat.gov.in

Abstract:
In this article, Physics and Technology of Semiconductor Optoelectronic Devices that are recently developed at RRCAT is briefly described. Semiconductor heterostructures, quantum-well, quantum-dot, and dot-in-well structures of excellent quality are grown by using the metal organic vapour phase epitaxy at RRCAT. A methodology for growing high quality III-V semiconductor hetero and nanostructures on group IV substrates is also investigated by understanding the role of surface energy. Subsequently, an in-depth investigations of these structures is performed by using laboratory and synchrotron radiation based facilities. Fundamental physics issues related to the confinement effect on the effective mass of excitons in quantum structure are investigated using the contactless magneto-photoluminescence technique. Presence of carrier localization leading to "S-shaped" temperature dependence of PL peak energy is explained which enabled an accurate measurements of the exciton localization energy and material parameters of QWs wherein the conventional models of Varshni, Viña and Passler failed. Further, the role of exciton localization on the quantum efficiency and operating temperature range of quantum well infrared detectors is identified and explained. The new sets of multilayer materials ZrO_2 and ZrO_2/SiO_2, having high damage threshold of the cavity mirrors are investigated for facet coting of laser diode arrays. Semiconductor laser diode arrays, and radiation resistant quadrant GaAs detectors are developed at RRCAT. The laser diode arrays operating at 980nm delivered 23.5 W peak power under pulsed operation and 3 W CW power. Similarly, radiation resistant quadrant detectors consisting of 4 active elements of GaAs based structures that operate in the wavelength range of 200-900 nm are also developed. The detector can be used in precise alignment of laser and charged particle beams in high radiation zones due to high radiation hardness of GaAs compared to Si.

1. Introduction: In this article, physics of semiconductor materials and devices that are indigenously developed at RRCAT is briefly described. Semiconductor heterostructures, quantum-well (QW), quantum-dot (QD), and dot-in-well (DWELL) structures of excellent quality are grown by using the metal organic vapour phase epitaxy technique at RRCAT [1-9]. A methodology for growing high quality III-V semiconductor heteroand nanostructures on group IV substrates is investigated by understanding the role of surface energy between the grown layer and substrates at the optimized kinetics[10-16]. Subsequently, an in-depth investigation of the grown semiconductor structures is performed by using the laboratory and synchrotron radiation based facilities [17-21]. Presence of carrier localization leading to "S-shaped" temperature dependence of PL peak energy is explained which enabled an accurate measurements of the exciton localization energy and material parameters of QWs wherein the conventional models of Varshni, Viña and Passler failed [22]. The role of exciton localization on the quantum efficiency and operating temperature range of quantum well infrared detectors is identified and explained [23,24]. The microscopic properties of exciton, such as effective mass, binding energy, Bohr radius, for semiconductor quantum structures are obtained from a contact less magneto-PL spectroscopy [25,28]. Influence of ultra-low defects and atomic irregularities at the hetero-junction on the optical properties of free and bound excitons are also investigated by the Magneto Photoluminescence spectroscopy[27-28]. The multilayer materials of ZrO_2 and ZrO_2/SiO_2 are investigated for antireflection (AR) and high reflection (HR) coatings [29]. The promising properties of the materials confirms that they can be deployed for fabricating the semiconductor device. Subsequently, Semiconductor laser diode arrays & radiation resistant quadrant GaAs *p-i-n* and quantum well detectors devices are developed [29-32].

2. Growth of Semiconductor Structures: All the semiconductor structuresare predominantly grown on nominally (001) oriented n^+-GaAs or n^+-InP and their semisulating substrates using horizontal low-pressure MOVPE reactor with a rotating substrate holder. Trimethyl Gallium, Trimethyl Indium and Trimethyl Aluminium are used as precursors for group III elements while 100% Arsine and Phospine are used for group V elements. Dimethyl Zinc and 2% SiH_4 in H_2 are used as the dopant source for *p* and *n* type carriers respectively. The V/III ratio remains ~ 100 for most of the growth except for InAsP where it changed to ~ 235. Growth temperature is optimized for the individual layer and it remains within the range of 400 to 770 ^{o}C for different layers. The thickness, carrier types and their density in the buffer, cap and active layers are optimized as per the planned device structures or the kind of investigations. Subsequently, numerous single, multiple quantum wells and surface quantum wells are grown as per the theoretical design. Typical device structures along with their energy band structures are shown in the *Fig.T.1.1*. The laser diode structure consists of AlGaAs based cladding layer, graded refractive

index layer, waveguide layer and the active region which is a double quantum well structure (*Fig. T.1.1a*). The GaAs detector structures consists of ~ 4 µm thick intrinsic GaAs layer (*i*) is sandwiched between 300 nm of p type (p ~ 3 x 10^{18} cm^{3}) and 300 nm of n type (n ~ 2 x 10^{18} cm^{3}) GaAs layers to form the *p-i-n* detector structure (*Fig.T.1.1b*). Similarly, quantum well and quantum dot in well structures are also grown and their MESA sturture based devices are also fabricated (*Fig. T.1.2a & b*) [1-9].

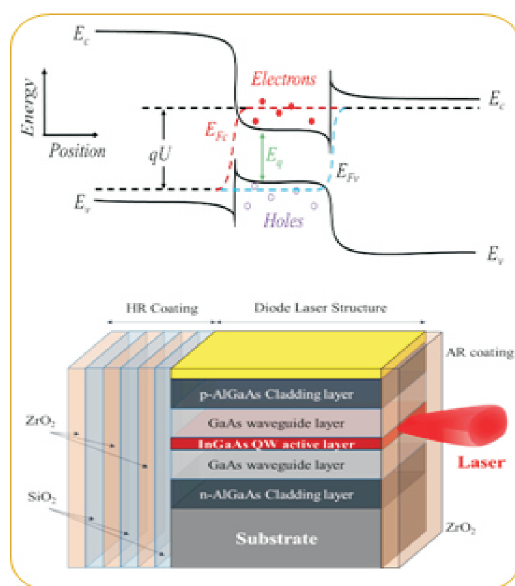

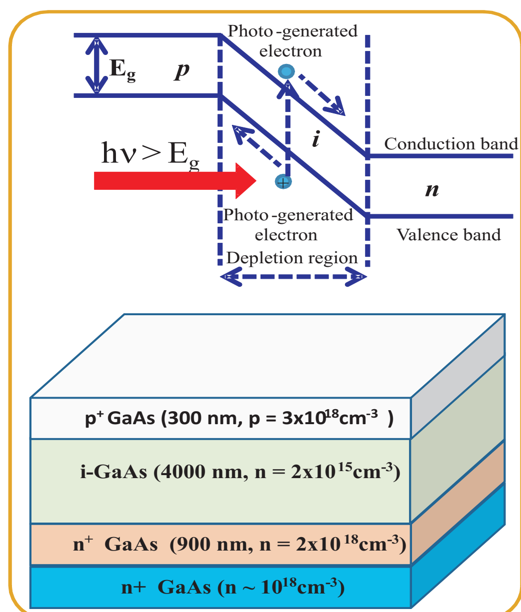

Fig. T.1.1:Schematic of the device structures grown by using MOVPE, a) Laser diode[29] (b) p-i-n detector[30-32]

Further, in order to meet the future requirement for the development of high efficiency multijunction solar cells, advanced lasers, wide range of detectors, and spin-photonic devices, high quality III-V structures need to be integrated on Si and Ge substrates. However, it is not trivial due to the incompatibility between respective material properties such as interfacial hetero-valency (polar/non-polar), lattice mismatch, surface and interfacial chemistry. In spite of these limitations, we have achieved successful growth of GaP and GaAs on Si and Ge using the two step growth procedure based on the nucleating layer and thick layer concept [1,11-12].

3. Experiment & Analysis: *A. Structural*: In-depth information of the grown structures are obtained by using numerous experiments using laboratory and synchrotron radiation based facilities.

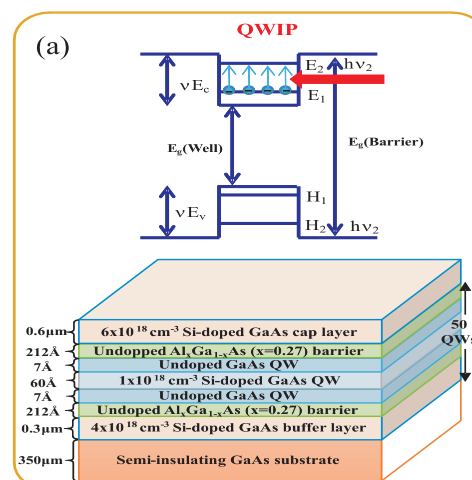

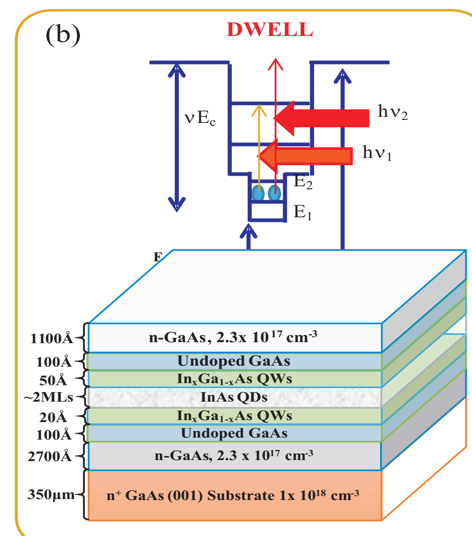

Fig. T.1.2: Schematic of quantum well (a) and quantum dot in well (b)structures grown by using MOVPE[4,5]

The structural parameters, such as thickness, composition and strain, of the grown layer and structures are determined from high resolution x-ray diffraction (HRXRD)[1-9]. These parameters are obtained from the well-defined pendellosung fringes observed in the HRXRD profile by matching the experimental and simulated diffraction patterns [1-9].Typical HRXRD patterns for one of the strained and relaxed structures are shown in the *Fig.T.1.3a & b*. The nature of strain and its distribution in the grown structures are identified from the reciprocal space map (RSM) obtained by measuring a series of ω-2θ scans each having a different ω offset. Typical RSM profile of completely strained (InAsP/InP) and fully relaxed structures (GaP/Ge) in the reciprocal space coordinates (q_x, q_z) are shown in the *Fig.T.1.3a & b* respectively.

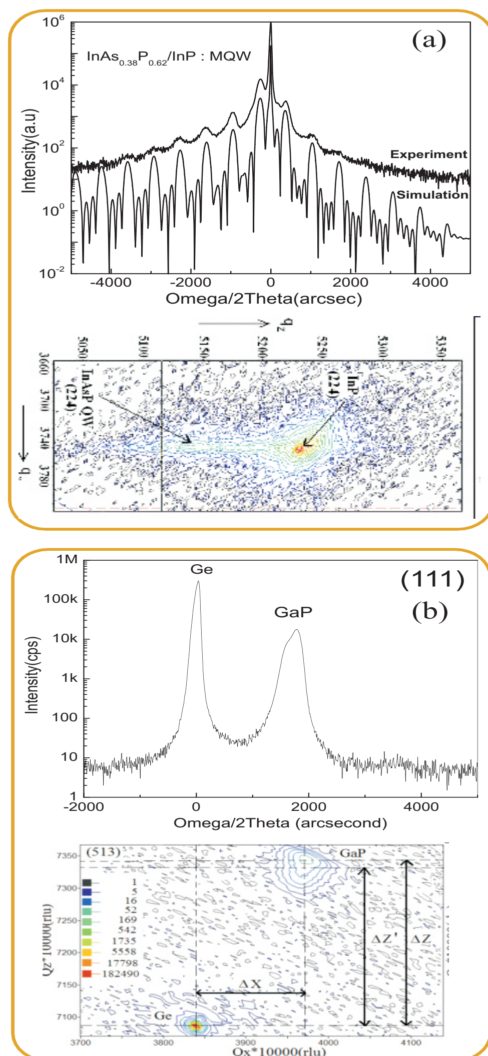

Fig. T.1.3:Typical HRXRDprofile of ω-2θ *and area scans of strained(a) and relaxed (b) structures[1,3].*

From the symmetric/asymmetric contour lines one can estimate the strain distribution nature. In-plane strain ($\varepsilon^{\parallel}$) and the strain along perpendicular direction (ε) are estimated by using the expressions $\varepsilon^{\parallel} = X/(X_s\text{-}X) = (a_L^{\parallel}\text{-}\ a_s)/a_s$ and $\varepsilon = Z/(Z_s\text{-}Z) = (a_L - a_s)/a_s$, where X_S (X_L) and Z_S (Z_L) indicate the reciprocal lattice point for substrate (epilayer) along the q_X and q_Z directions of the asymmetric RSM plot, respectively. The interfacial quality between the layers and their thickness are also verified from the cross-sectional TEM micrographs and they are in agreement with that obtained by HRXRD [1]. *Figure T.1.4a, b&c* shows a typical TEM image of QWs, MQW& DWELL structures [3,4]. The distributions of the QDs sizes and their morphology are also investigated on uncapped InAs QDs using AFM[4]. QD density of ~ 7.2x $10^9/cm^2$ is estimated from AFM image of uncapped QD structure[4].

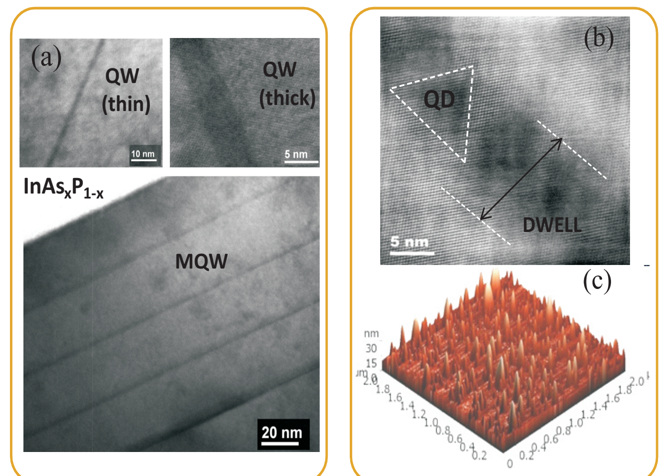

Fig. T.1.4:Cross-sectional TEM images of thin & thick QWs, MQWs (a) and DWELL showing QDs(b),AFM image of QDs(c).

The interface roughness between the oxide multilayers that are used for antireflection and high reflection coatings on the devices structures are evaluated using x-ray reflectivity (XRR) by Hard/soft x-ray beam of CuKα lab source/synchrotron radiation source at Indus-1 synchrotron beamline facility respectively. In the Indus-1 beamlines, photons of the wavelength of 80, 100, 120 and 130 Å are used to illuminate the sample and reflectivity data is recorded from 0–70° incidence angle. Initially XRR measurements are performed using hard X-ray source i.e. CuKα. Thickness of each individual layer, density profile, surface and interface roughness are determined by fitting the experimental XRR pattern by using the Parratt recursion formula. Typical electron density profile (δ_e) of ZrO_2 /GaAs layer is shown in

the inset of *Fig. T.1.5a*. It is evident from the $_e$ profile that the layer is uniform across the depth except near the surface (air/ZrO_2) and ZrO_2 layer/substrate interface. Further, the optical density (δ_{op}) and absorption coefficients (β) are also measured by wavelength dependent (80, 100Å) soft x-ray measurements using synchrotron x-rays source. *Fig. T.1.5b* shows the experimental and fitted reflectivity profiles of ZrO_2/GaAs single layer. The values of δ_{op} and β measured using 100 Å wavelength are 2.45×10^{-2} and 2.78×10^{-3} respectively for ZrO_2 layer which closely matches with that of the bulk values of ZrO_2 (2.8×10^{-2}, 2.78×10^{-3}). Similarly the values of δ_{op} and β measured using 80Å for the same ZrO_2 layer are 1.33×10^{-2} and 2.38×10^{-3} respectively that are closely matching with the values of bulk ZrO_2 material which are 1.69×10^{-2}, and 3.77×10^{-3} respectively. Further, δ_{op} profiles obtained from the fitting of soft XRR pattern are shown in the inset of *Fig. T.1.5b*.

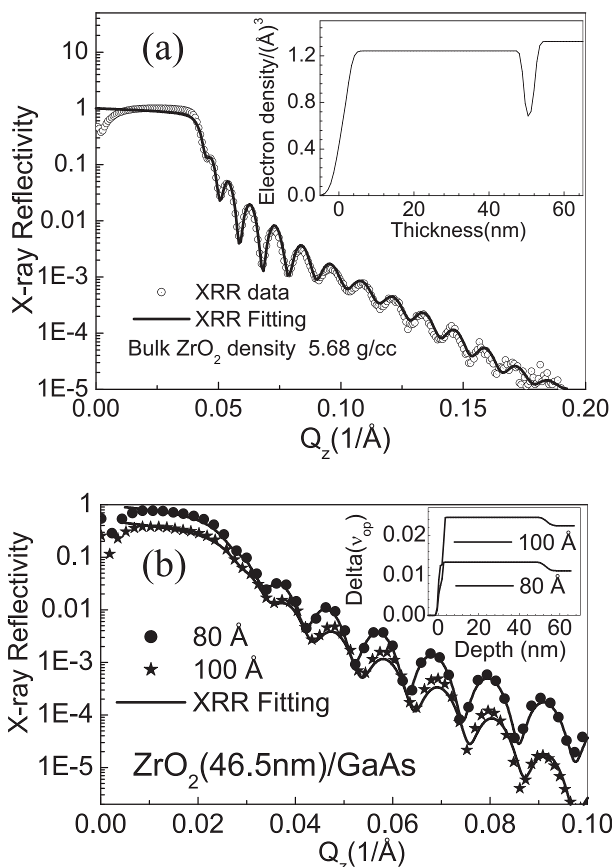

Fig. T.1.5: The experimental and simulated x-ray reflectivity of ZrO_2/GaAs with a) Hard X-ray, CuK$_\alpha$source and electron density profile b) Soft X-ray energies and optical density profiles.

Thus δ_{op} profile also confirms that the ZrO_2 layer is highly uniform and sandwiched between a top surface layer and a bottom native oxide layer on the substrate. Similarly, several parameters of the grown semiconductor layers are obtained using an angle integrated photoelectron spectroscopy (PES) and angle resolved photoelectron spectroscopy (ARPES) beam lines at Indus-I synchrotron radiation source with a photon energy of 100 and 180 eV[1,11,27]. From these measurements and analysis it is concluded that the semiconductor layers, quantum structures and Oxide layers are of excellent quality. However, all these techniques do not predict directly the influence of ultralow defects on the opto-electronic properties of the grown materials. In contrast, contactless PL and surface photo-voltage (SPV) spectroscopy are more effective techniques for studying the optical quality and also the defects. Localization of charge carrier and their dynamics are explained from the temperature dependent conventional emission and absorption based PL and SPV process.

B. Photoluminescence analysis: Power and temperature dependent : In order to investigate the carrier emission and recombination mechanism in the grown structures, power and temperature dependent photoluminescence are performed. The origin of experimental emission energies are explained from the theoretical values obtained by solving the Schrodinger equation using finite difference approach within an envelope-function formalism framework. Generally, it is observed that the radiative recombination efficiency of AlGaAs/GaAs QW samples is highfor the same power density of excitation [25].

It is also observed that almost all the QWs show monotonic decrease in transition energy with rise in temperature. However at low temperatures, these QWs show different temperature dependent behavior (*Fig. T.1.6a & b*). This behavior is different for different level of illumination power. The structures with ternary materials in QWs mostly show anomalous S (red-blue-red) shaped energy versus temperature behavior (*Fig. T.1.6b*), while samples with binary material in the QW region does not show such behavior (*Fig. T.1.6a*). The S-shaped temperature dependence of ground state transition energy is explained by considering the charge carrier localization in the band-tail states where the ground state energy follows the temperature dependence of the localization states. One therefore sees a normal temperature induced bandgap shrinkage (red shift) up to the critical temperature which is mainly governed by the localization energy. At a critical temperature, excitons having sufficient thermal energy enabling their delocalization which leads to the dominance of band to band exciton feature.

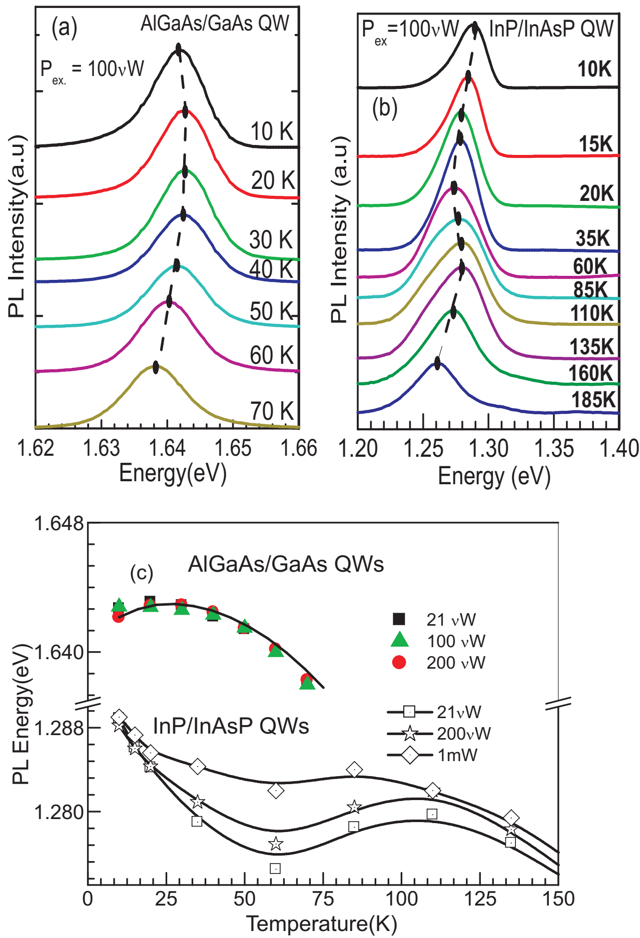

Fig. T.1.6: Temperature dependent PL spectra of QWs (a) AlGaAs/GaAs (b) InP/InAsP, (c) Power and temperature dependent energy band gap variation for AlGaAs/GaAs & InP/InAsP QWs.

Because of this, the energy of ground state feature increases (blue shift) until the localized exciton feature starts to weaken upto critical temperature (*Fig T.1.6c*). Above this temperature, excitons are in thermal equilibrium and once again one sees the usual temperature induced bandgap shrinkage (red shift) up to room temperature. At reasonably high excitation intensities, a large numbers of electron-hole pairs are generated which lead to the saturation of band tail states that reduces the effect of carrier localization because of the limited density of localized states. Under such condition, though the band to band recombination dominates over the localized states recombination but they influence the luminescence spectra significantly. In such a situation conventional models of Varshni, Viña and Passler break down, where Dixit et al.[22] have proposed a phenomenological model for evaluating the material parameters and localization energy of carriers trapped in the band-tail states as given below,

$$E_{PL}^{Peak} = \frac{n_1}{n_1+n_2} E_g^{QW}(0) + \frac{n_2}{n_1+n_2} E_t - F(T) \quad (1)$$

where E_{PL}^{Peak} is the PL peak energy at a given temperature, n_1 and n_2 are the associated weighting factors which tells if either the transitions are band-to-band dominated or the localized exciton dominated at energy $E_g^{QW}(0)$ and $E_t(0)$ respectively [22]. Here, F(T) is the temperature dependent term which takes into account the electron-phonon interaction and thermal expansion of the lattice parameters. If the fraction (p) is defined in terms of weighting factors as $p = n_2/(n_1+n_2)$ then equation 1 can be rewritten as,

$$E_{PL}^{Peak} = (1-p)\, E_g^{QW}(0) + pE_t - \frac{\alpha T^2}{\beta + T} \quad (2)$$

The material parameters (α, β) and localization energy ($\Delta E = E_g^{QW}(0) - E_t$) for all the QW samples showing such behavior can be obtained. Here, α tells the disorders or entropy of the system while β is related to Debye or phonon temperature. Thus for ternary QWs system using above process one can estimate the trap energy values and materials parameters which can also give information of disorders in the systems. It is further explained how the magnitude of charge carrier localization energy influences the critical temperature of S-shaped temperature dependent energy variation. It is also proposed a methodology to extract the value of carrier localization energy directly from temperature dependent SPV and PC [23,24]. This information can play a pivotal role in defining the operating temperature range of absorption based quantum structures devices, where such S-shaped behaviour of excitonic transition energy is observed.

C.Magnetic field dependent: In order to investigate the microscopic properties of exciton, such as effective mass, binding energy, Bohr radius and ultralow disorders for semiconductor quantum structuresMagneto-PL measurement are performed.In this experiment, the sample is mounted horizontally in the VTI assembly and field is applied along the growth direction, known as Faraday geometry, and excitonic properties are probed in the plane of the sample. Under this condition the magnetic field driven confinement of charge carrier at high field produce discrete harmonic oscillator like Landau energy levels which blue shift with field. From the blue shift we have estimated the effective mass of charge carriers [25-28].

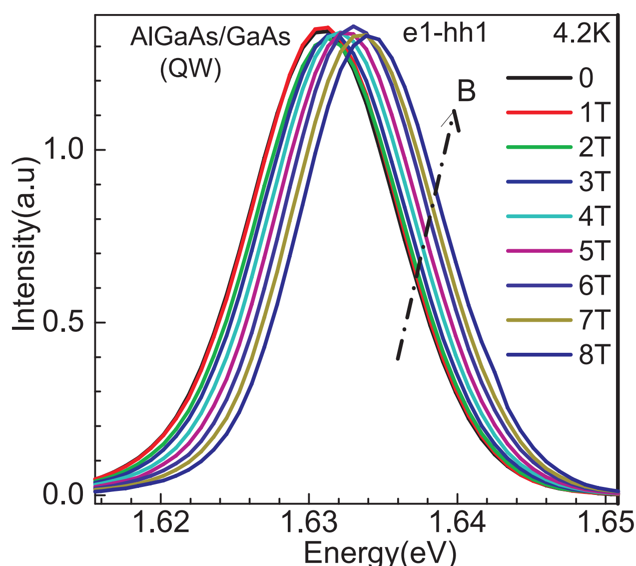

Fig. T.1.7: Magneto-PL spectra of AlGaAs/GaAs QWs

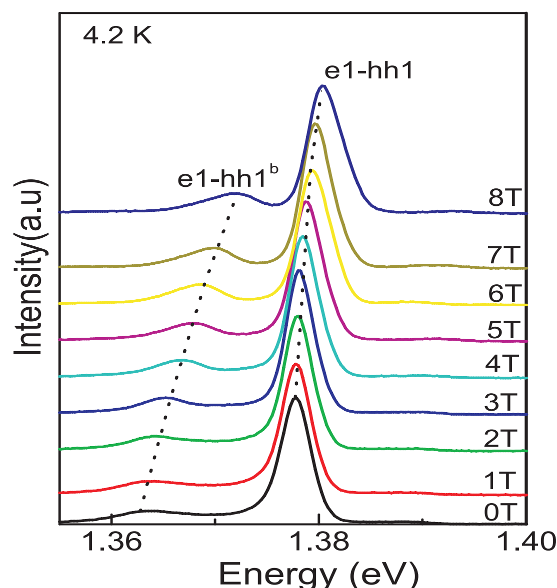

In addition, the sample is also mounted vertically in the VTI and field is applied perpendicular to the growth direction, known as Voigt geometry and the extent of the wave function in growth direction is probed for studying the electronic coupling of stacked quantum structures. It is observed that the spectrum of all the samples show blue energy shift with applied magnetic field due to the predominant contributions of diamagnetic and Landau shifts (*Fig.T.1.7*).The magnetic field dependent diamagnetic blue shift of PL spectra is proportional to the square of B ($B < B_c$). However, at relatively higher magnetic field, excitons are confined to small radius. This magnetic field driven in plane confinement of exciton (in x-y plane) is responsible for the formation of discrete Landau levels.In this region ($B \geq Bc$), blue shift in energy levels become proportional to the applied field B. The magnetic field, above which magnetic energy becomes dominant over Columbic energy, is termed as critical magnetic field and is theoretically estimated as 4.9 T for GaAs. Significant increase of effective mass is observed for the confined exciton in narrow QWs. The reason behind such an observation is due to the induced non-parabolicity in bands [26-28]. Similarly, In order to obtain such results on the laser diode structure, we have performed similar experiment and observed interesting results which are discussed below.It is observed that the luminescence spectrum of LD structure at low temperature show strong influence of carrier localization [25].

Fig. T.1.8 show the magneto-PL spectrum of laser diode structure.

The transition energy of localized peak (e_1-hh_1^b) and band to band (e_1-hh_1) peak blue shift with applied magnetic field. The shift for localized peak (e_1-hh_1^b) is significantly higher (10 meV) then band to band (e_1-hh_1) peak (3 meV). This observation confirms that charge carrier gets redistributed among the localized states and give rise to higher energy shift with field. Similarly, under the extreme perturbation, like high electric field or current, carriers gets redistributed among these states and therefore may affect the operating wavelength of the devices [25].

4. Devices processing, packaging and testing:

Promising properties of the investigated materials ensured to fabricate the useful devices. Subsequently, the MOVPE grown laser diode structures are processed through conventional optical lithography, n- and p-type metal contact formation by e-beam/thermal evaporation, lift-off process and rapid thermal annealing. After making a smooth walled mesa structure using H_3PO_4:CH_3OH:H_2O_2 etchant solution, electrical isolation and side-wall passivation is realized by SiO_2 layer deposition between the metal stripes. Finally, the structure is thinned down to ~140 µm and several laser elements of 500 µm cavity length and 100 µm strip width are cleaved. Subsequently, antireflection and high reflection coatings of ZrO_2 based multilayers deposited on the facets of

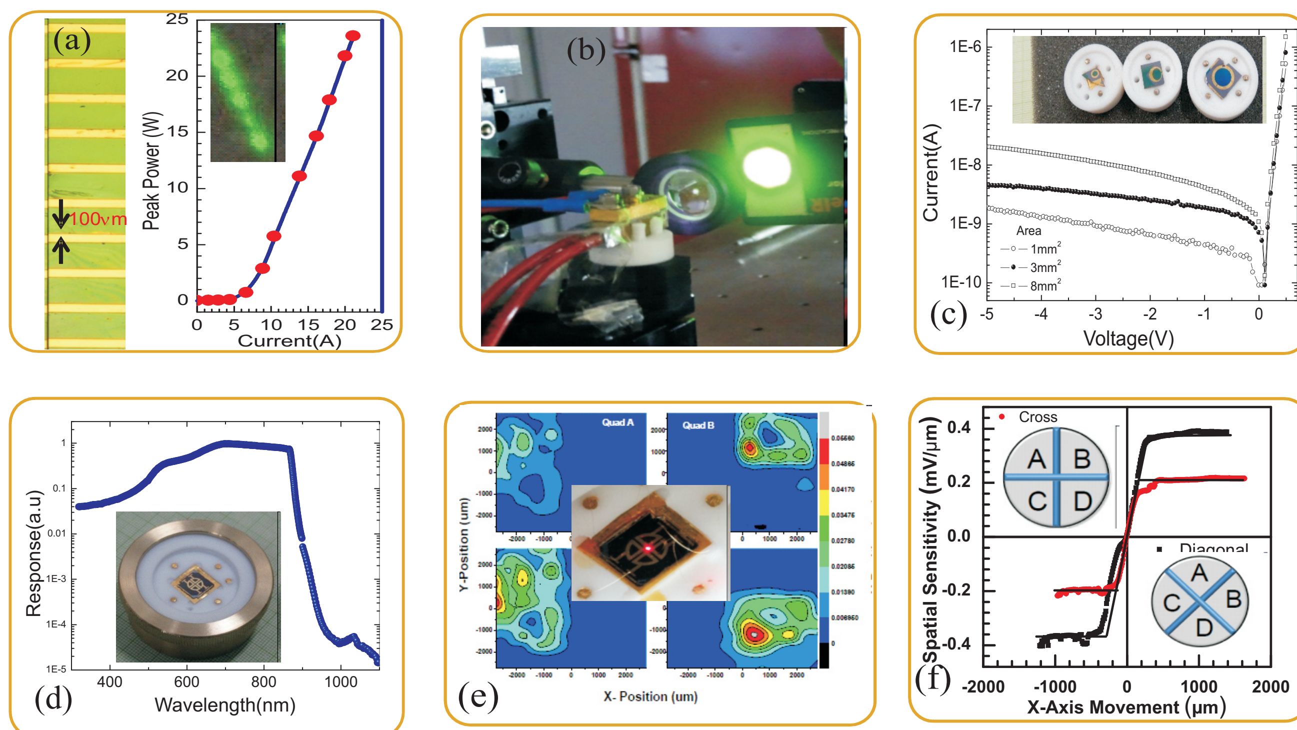

Fig. T.1.9: Photograph of laser diode arrays and its L-I characteristics. b) Photograph of a 980 nm laser diode array under operation. c) I-V characteristics & photograph of developed detector d) Optical response of the developed quadrant detector along with photograph e) Laser beam profiling using indigenously developed detector f) Position sensitivity of the detector in two geometry.

laser diodes using e-beam evaporation. Further, we optimized the high power laser diode die bonding process with two different types of solder material/s namely Indium preform (soft solder) and Gold-Tin (AuSn-hard solder). The devices are bonded on gold plated Copper and KOVAR substrates.

Finally, the laser diode arrays emitting at ~ 980 nm consists of more than 10 elements are bonded and packaged on water cooled micro-channel laser mounting assembly. These laser diode arrays were successfully operated at 23.5 W peak power with 5.65 ms pulse width at 1 Hz rep rate (Fig. T.1.9a & b).These laser diode arrays also delivered 3 W output power under CW mode.Similarly, GaAs p-i-n detector structure are processed using two sets of metal shadowmasks, one for defining the electrode area and the other for the surface passivation of detector structure. For theprocessing of devices, first n-side electrode is formed using multilayer coating of Au-Ge/Ni/Au metals on the back side of GaAs substrate and subsequent rapid thermal annealing (RTA) at ~ 450°C for 50 sec in nitrogen ambient. Subsequently, p-side metal electrode (ring type) is formed using one set of metal mask by multilayer evaporation of Ti/Pt/Au metals and subsequent RTA process. The current spreading area from the top of the device region is removed by chemical etching process. Thereafter, the surface area of the detector is passivated by SiO_2 dielectric which is deposited by e-beam evaporation method using the second set of metal mask. Gold wire of ~25 µm diameter is used for ball bonding on the p-side electrode (Ti/Pt/Au). Silver paste is used for n-side contact formation with the back side of GaAs substrate. The best detectors with area of 1mm^2, 3 mm^2 and 8 mm^2 showed 1.5 nA, 4.5 nA and 10 nA dark current at roomtemperature respectively(Fig. T.1.9c). Further, we have also developed GaAs based quadrant detectors. These radiation resistant quadrant detectors consisting of 4 active elements of GaAs based p-i-n structures that operate in the wavelength range of 200-900 nm are used for the precise alignment of laser beam with ~50 µm spatial resolution(Fig. T.1.9d & f).

5. Conclusion:

In this article physics and applications of semiconductor quantum structures that are accomplished at RRCAT are briefly described. Semiconductor heterostructures, quantum-

well, quantum-dot, and dot-in-well structures of excellent quality are grown by using MOVPE. A methodology for growing high quality III-V semiconductor heterostructures and nanostructures on group IV substrates is also investigated by understanding the role of surface energy. The role of charge carrier confinement on the effective mass of excitons in quantum structure are investigated using non-contact based magneto photoluminescence. Presence of carrier localization leading to "S-shaped" temperature dependence of PL peak energy are explained and modeled which enabled an accurate measurements of the exciton localization energy and material parameters of QWs wherein the conventional models of Varshni, Viña and Passler failed. Further, the role of such localization on the quantum efficiency and operating temperature range of quantum well infrared detectors is identified and explained. Properties of new sets of multilayer materials ZrO_2 and ZrO_2/SiO_2 are investigated for facet coating which assured to have increased the damage threshold of laser diode arrays. The processed laser diode emitting at ~ 980nm, is operated under CW mode with total output power of 0.75 W from the facet coated laser diode with ~ 52% wall plug efficiency. Subsequently, laser diode arrays are also developed which delivered 23.5 W peak power under pulsed operation and 3 W CW power. These bonded and packaged laser diode can be used for investigating the material parameters and the same is proven by using it as a pump source in the photoluminescence experiments. Similarly, radiation resistant quadrant detectors, consist of 4 active elements of GaAs based structures, operate in the wavelength range of 200-900 nm are also developed. The detector can be used in precise alignment of laser and charged particle beams in high radiation zones due to high radiation hardness of GaAs compared to Si.

Acknowledgments:

Author acknowledge Shri U. K. Ghosh, Shri A. Jaiswal and Shri G. Jayaprakash for the technical support. Authors also acknowledge Dr. T. K. Sharma, Dr. A. Chakrabarti, Dr. T. Ganguli, Dr. C Mukherjee, Dr. B. N. Upadhay, Dr. P. K. Mukhopadhaya, Dr. S. Pal, Dr. S. D. Singh, Mr.S. Khamari, Mr. R. Jangir, Ms. Geentanjali, Mr. S. Haldar, Mr. R. Roychowdhury, Mr. R. Kumar, Mr. S. Porwal, Mr. V. Agnihotri, Dr. K. S. Bindra and Dr. S. M. Oak for their useful contributions in this work. Author also acknowledge Shri P. K. Kush for providing adequate liquid Helium for Magneto-PL experiment. Author also acknowledge Dr. R, Chari, Dr. Bindra, Dr. P. A. Naik, Director RRCAT, & Dr. P. D. Gupta, formar director of RRCAT, for their constant support during the course of this work.

References:

1. V. K. Dixit, Shailendra Kumar, S. D. Singh, S. K. Khamari, R. Kumar, Pragya Tiwari, D. M. Phase, T. K. Sharma, and S. M. Oak, Investigation of crystalline and electronic band alignment properties of GaP/Ge(111) heterostructure" Appl. Phys. Lett. 104, 092101 (2014).

2. V. K. Dixit, Shailendra Kumar , S.D. Singh, S. Porwal, T.K. Sharma, S.M. Oak, "Band alignment and quantum states of $InAs_xP_{1-x}/InP$ surface quantum wells investigated from ultraviolet photoelectron spectroscopy and photoluminescence", Materials Letters 87, 69 (2012).

3. V. K. Dixit, S. D. Singh, S Porwal, R. Kumar, A K Srivastava, Tapas Ganguli, T. K. Sharma and S M Oak, "Determination of band offsets in strained $InAs_xP_{1-x}/InP$ quantum well by capacitance voltage profile and photoluminescence spectroscopy", J. Appl. Phys. 109, 083702 (2011).

4. V. K. Dixit, Shailesh K Khamari, C Tyagi, S D Singh, S Porwal, Ravi Kumar, C Mukherjee, P Mondal, A K Srivastava, T K Sharma and S M Oak, "Evaluation of electronic transport properties and conduction band offsets of asymmetric $InAs/In_xGa_{1-x}As/GaAs$ dot-in-well structures", J. Phys. D: Appl. Phys.45, 365104(2012).

5. V. K. Dixit, S. D. Singh, T. K. Sharma, Tapas Ganguli, Suparna Pal, B. Q. Khattak and S. M. Oak. "Studies on GaAs/AlGaAs based (p and n-type) quantum well infrared photodetector structures grown using metal organic vapour phase epitaxy" IEEE Xplore, 9858874, 355, (2008).

6. S. D. Singh, V. K. Dixit, S. Khamari, R. Kumar, A K Srivastava, Tapas Ganguli, and S M Oak, "Conduction band offset and Quantum states probed by capacitance-voltage measurements for InP/GaAs type-II ultrathin quantum wells", J. Appl. Phys. 109, 073702, (2011).

7. S. D. Singh, V. K. Dixit, S. Porwal S., R. Kumar, A. K. Srivastava, T. Ganguli, T. K. Sharma and S. M. Oak, "Observation of electron confinement in InP/GaAs type-II ultrathin quantum wells", Appl. Phys. Lett., 97, 111912, (2010).

8. S. D Singh, S. Porwal, K. Alexander, V. K. Dixit., A. K. Srivastava and S. M. Oak, "Temperature dependence of the photoluminescence from InP/GaAs type-II ultrathin

quantum wells", J. Phys. D: Appl. Phys., 43, 455410, (2010).

9. S D Singh, S Porwal, Puspen Mondal, AK Srivastava, C Mukherjee,V. K. Dixit, T. K. Sharma, S. M. Oak, Observation of room temperature optical absorption in InP/GaAs type-II ultrathin quantum wells and quantum dots", J. Appl. Phys. 115, 223505 (2014)

10. V. K. Dixit, "Challenges in the integration of III-V and III-V-N semiconductors on Si or Ge substrates" 20th National Seminar on Single Crystal Growth and Applications (NSCGA-2016), Mumbai, Jan.19-21, (2016) (Invited talk).

11. R. Roychowdhury, S. Kumar, A. Wadikar, C. Mukherjee, K. Rajiv, T. K. Sharma, and V. K. Dixit, "Role of surface energy on the morphology and optical properties of GaP micro & nano structures grown on polar and non-polar substrates" Appl. Surf. Science 419, 957 (2017)

12. V. K. Dixit, T. Ganguli, T. K. Sharma, S. D Singh, Ravi Kumar, S. Porwal, Alka Ingale, Pragya Tiwari, and S. M. Oak, "Effect of two step growth process on structural, optical and electrical properties of MOVPE grown GaP/Si". J. Crystal Growth, 310, 3428 (2008).

13. V. K. Dixit,T. Ganguli, T. K. Sharma, Ravi Kumar, S. Porwal, Vijay Shukla , Alka Ingale, Pragya Tiwari, and A. K. Nath, "Studies on MOVPE growth of GaP epitaxial layer on Si(001) substrate and effects of annealing"J. Crystal Growth, 5, 293, (2006).

14. S. Pal, V. G. Sathe, K. Rajiv, C. Mukherjee, R. Kumar, and V. K. Dixit, "Effect of surface morphology on the optical properties of InAs/Ge (111)" Appl. Surf. Science 372 70 (2016).

15. S. Pal, S.D. Singh, V.K. Dixit,T.K. Sharma, R. Kumar, A.K. Sinha, V. Sathe, D.M. Phase, C. Mukherjee, Alka Ingale, "Crystalline and band alignment properties of InAs/Ge (111) heterostructures" Journal of Alloys and Compounds 646, 393 (2015).

16. Low- and high-density InAs on Si(001) and their Raman imaging" Suparna Pal, S.D. Singh, V. K. Dixit, Alka Ingale, Pragya Tiwari, Himanshu Srivastava, Ravi Kumar, C. Mukherjee, P. Prakash and S. M. Oak, , Semicond. Sci. Technol., 28, 015025 (2013).

17. R. Kumar, T. Ganguli, V. Chouhan, V. K. Dixit, Puspen Mondal, A.K. Srivastava, C. Mukherjee, T.K. Sharma, Evaluation of Vertical Coherence Length, Twist and Microstrain of GaAs /Si Epilayers" using modified Williamson-Hall Analysis, J. Nano - Electron. Phys. 2, 02010 (2014).

18. R. Kumar, T. Ganguli, V. Chouhan and V.K. Dixit, "The study of microstructure of III-V polar on non-polar heterostructures by HRXRD" J. Nano- Electron. Phys. 3, 17 (2011).

19. S. Kumar, C. Mukherjee, V. K. Dixit, S. D. Singh and S.N. Jha, Ultraviolet Photoelectron Spectroscopy of Nano In Clusters Schottky Barriers on Sputtered InP" Appl. Surf. Science, 258, 143, (2011).

20. R. Kumar, V. K. Dixit, T. Ganguli, C. Mukherjee, A.K. Srivastava, and T. K. Sharma, Observation of anisotropic distribution of microstructure in GaP/GaAs epitaxial layers"J. Appl. Phys. 120, 135307 (2016).

21. R. Kumar, V. K. Dixit, A. K. Sinha, T. Ganguli, C. Mukherjee, S. M. Oak, T. K. Sharma, Study of the microstructure information of GaAs epilayers grown on silicon substrate using synchrotron radiation, J. Synchrotron Radiat. 23, 238 (2016).

22. V. K. Dixit, S. Porwal, S. D. Singh, T. K. Sharma, S. Ghosh, S. M. Oak, A versatile phenomenological model for the S-shaped temperature dependence of photoluminescence energy for an accurate determination of the exciton localization energy in bulk and quantum well structures", J. Phys. D: Appl. Phys. 47, 065103 (2014).

23. Geetanjali Vashisht, V. K. Dixit, S. Porwal, R. Kumar, T. K. Sharma and S. M. Oak, "Effect of charge carrier localization on the quantum efficiency and operating temperature range of $InAs_xP_{1-x}$/InP quantum well detectors" J. of Applied Physics 119, 095708 (2016).

24. Geetanjali Vashisht, S. Porwal, R. Kumar, V. K. Dixit, T. K. Sharma and S. M. Oak "Development and application of InAsP/InP quantum well infrared detector", Geetanjali, AIP Conf. Proc. 1731, 120033 (2016).

25. V. K. Dixit, "Investigations on the complexities in active region of quantum well laser diode arrays" 25th National Laser Symposium (NLS-25), December, (2016) (Invited talk), KIIT, Bhubaneswar, India.

26. S. Haldar, G. Vashisht, S. Porwal, S. K. Khamari, V.K. Dixit, T. K. Sharma and S. M. Oak, “Role of disorder and multi-valley scattering on the dynamics and effective mass of excitons in $Al_xGa_{1-x}As$/GaAs quantum wells investigated by magnetophotoluminescence” Condensed Matter Physics under Extreme Conditions (CoMPEC-2016), BARC, Mumbai.

27. S. Haldar, V. K. Dixit, G. Vashisht, S. K. Khamari, S. Porwal, T. K. Sharma and S. M. Oak,Effect of carrier confinement on effective mass of excitons and estimation of ultralow disorder in $Al_xGa_{1-x}As$/GaAs quantum wells by magneto-photoluminescence" NATURE SCIENTIFIC REPORTS (2017)(In press).

28. S. Haldar, V. K. Dixit, G. Vashisht, S. Porwal andT. K. Sharma, Effect of magnetic field on free and bound exciton luminescence in GaAs/AlGaAs MQW structure : A quantitative study on the estimation of ultra-low disorder", J. Phys. D: Appl. Phys.,(2017)(In press).

29. V. K. Dixit, A. Marathe, G. Bhatt, S. K. Khamari, K Rajiv, R Kumar, C Mukherjee, C. J. Panchal, T K Sharma and S M Oak, “Evaluation of structural and microscopic properties of tetragonal ZrO_2 for the facet coating of 980 nm semiconductor laser diodes” J. Phys. D: Appl. Phys. 48, 105102, (2015).

30. V.K. Dixit, S. K. Khamari, S. Manwani, S. Porwal, K. Alexander, T. K. Sharma, S. Kher, S.M. Oak “Effect of high dose gamma-ray irradiation on GaAs *p-i-n* photodetectors”; Nuclear Instruments and Methods in Physics Research A 785, 93, (2015).

31. V. R. V. Pillai, S. K. Khamari, V. K. Dixit, T. Ganguli, S. Kher, S. M. Oak, “Effect of γ-ray irradiation on breakdown voltage, ideality factor, dark current and series resistance of GaAs *p–i–n* diode” Nuclear Instruments and Methods in Physics Research A, 685, 41, (2012).

32. S. K. Khamari, V. K. Dixit, T. Ganguli, S. Porwal, S.D. Singh, Sanjay Kher, R.K. Sharma, S.M. Oak, Effect of ^{60}Co γ-ray irradiation on electrical properties of GaAs epilayer and GaAs *p–i–n* diode” Nuclear Instruments and Methods in Physics Research Section B, 269, 272 (2011).